Radiology: Cardiothoracic Imaging

REVIEW

Vascular Malformations and Tumors: A Review of Classification and Imaging Features for Cardiothoracic Radiologists

Yoshiaki Ota, MD, PhD • Elizabeth Lee, MD • Edith Sella, MD • Prachi Agarwal, MD, MBBS

From the Division of Cardiothoracic Radiology, Department of Radiology, University of Michigan, 1500 E Medical Center Dr, Ann Arbor, MI 48109. Received December 27, 2022; revision requested February 3, 2023; revision received May 2; accepted May 17. **Address correspondence to** Y.O. (email: *ootayoshiaki@gmail.com*).

Authors declared no funding for this work.

Conflicts of interest are listed at the end of this article.

Radiology: Cardiothoracic Imaging 2023; 5(4):e220328 • https://doi.org/10.1148/ryct.220328 • Content codes: CH VA

The International Society for the Study of Vascular Anomalies (ISSVA) classification is a comprehensive histology-based scheme that was updated in 2018. It is important for cardiothoracic imagers to understand this classification to ensure that accurate terminology is used and that archaic terms are avoided when vascular lesions are described. Knowledge of the various malformations (including common conditions, such as venous malformation, arteriovenous fistula, and arteriovenous malformation) and vascular tumors allows for timely diagnosis and appropriate management. This review describes various vascular anomalies, in accordance with ISSVA classification and terminology; highlights key imaging features associated with each; and discusses the role of different imaging modalities.

The International Society for the Study of Vascular Anomalies (ISSVA) classification system is a comprehensive scheme based on Mulliken and Glowacki's seminal work. Classification was updated in 2018 because of improved knowledge of diagnostic and genetic features of vascular entities (Table 1) (1,2).

Vascular anomalies are divided into two broad categories (3–5): malformations and tumors. Malformations are nonneoplastic structural abnormalities that the ISSVA subcategorizes into simple, combined, malformations of major named vessels, and malformations associated with other anomalies (3,5). Simple malformations include capillary, lymphatic, venous, and arteriovenous malformations (AVMs) and arteriovenous fistulae (AVF). Combined malformations include lesions with two or more components, such as capillary-venous and lymphatic-venous, and so forth. Malformations with an arterial component constitute high-flow anomalies (eg, AVM, AVF). Malformations of major vessels are known as *channel type* and can involve major lymphatics, veins, and arteries. In addition, vascular malformations may be part of a syndrome and associated with other anomalies, such as limb overgrowth or bone undergrowth.

Vascular tumors, in contrast to malformations, are neoplastic, grow independently of overall body growth, and can regress on their own. Pathologically, vascular tumors show increased proliferation rates of endothelial and vascular cells (6) and are classified as benign, locally aggressive or borderline, and malignant (3,5,7). Some tumors may be congenital and present at birth.

The new ISSVA replaces outdated terms with more accurate nomenclature. For instance, inaccurate terms, such as *lymphangioma*, *cystic hygroma*, and *cavernous hemangioma* have been eliminated. These are confusing misnomers because the suffix "oma" typically implies tumors rather than malformations. In the new classification, *lymphangioma* and *cystic hygroma* have been replaced by *lymphatic malformation*, and *cavernous hemangioma* has been replaced by *venous malformation*. Notably, incorrect usage of the term *hemangioma* for lesions that are more aptly classified as venous malformations is pervasive in clinical practice, medical literature, and scientific reports. Commonly encountered incidental liver and skeletal lesions are frequently mislabeled as cavernous hemangiomas instead of venous malformations. A study showed that *hemangioma* appearing in the title or abstract was incorrectly used about 60%–85% of the time (8). As a result, the new classification no longer classifies hemangiomas into capillary and cavernous but instead into infantile and congenital. Familiarity with the new ISSVA classification can help in unambiguous communication and appropriate management.

This review focuses on the imaging spectrum of thoracic vascular anomalies, emphasizes the need for appropriate nomenclature, and discusses the role of various imaging modalities (9).

Imaging Modalities

The choice of an imaging modality depends on lesion location, patient age, and local expertise. Vascular anomalies may be first detected on scans obtained for other reasons. Radiography has a limited role but may be the initial test for nonspecific symptoms.

US Imaging

US is useful for superficial vascular lesions and can be used to define anatomic location, compressibility, arterial and/or venous waveforms, whether the lesion is single or multifocal, and presence of soft-tissue component (10), without radiation, as well as to provide guidance for sclerotherapy. Transthoracic contrast-enhanced echocardiography can serve as a screening test in sus-

Abbreviations

AVF = arteriovenous fistula, AVM = arteriovenous malformation, GLUT-1 = glucose transporter 1, HHT = hereditary hemorrhagic telangiectasia, ISSVA = International Society for the Study of Vascular Anomalies, LM = lymphatic malformation, PAVM = pulmonary AVM, VM = venous malformations

Summary

Knowledge of the imaging features associated with vascular anomalies, as classified according to the 2018 International Society for the Study of Vascular Anomalies, will aid cardiothoracic radiologists in providing appropriate diagnoses.

Essentials

- Vascular malformations and tumors are classified according to the International Society for the Study of Vascular Anomalies classification.
- Use of the terms *lymphangioma*, *cystic hygroma*, and *cavernous hemangioma* should be avoided, and contemporary nomenclature (*lymphatic malformation* for *lymphangioma* and *cystic hygroma*; *venous malformation* for *cavernous hemangioma*) should be used to ensure appropriate management.
- US, MRI, and CT are the first-line modalities used to assess vascular malformations and tumors in the thorax for guiding diagnosis and treatment.

Keywords

Pulmonary, Soft Tissues/Skin, Vascular, Arteriovenous Malformation

pected pulmonary AVM (PAVM), especially in hereditary hemorrhagic telangiectasia (HHT), given its high sensitivity and low risk; however, CT is recommended for confirmation of the diagnosis (11).

MRI Scan

MRI is often the test of choice because of its superior soft-tissue characterization (12,13) and is helpful in diagnosis, evaluating extent, and treatment planning. Starting with coronal or sagittal (depending on lesion location) T2-weighted imaging can aid in understanding lesion extent and can be used to tailor the remainder of the examination to ensure adequate coverage (14). This strategy can minimize the need for repeat axial imaging due to incomplete coverage.

Time-resolved contrast-enhanced MR angiography and venography are useful in demonstrating arteriovenous shunting, enhancement dynamics, and anatomy (2,14).

CT Imaging

CT can be used for diagnosis, localization, and treatment planning of vascular anomalies (15), especially if they are suspected in the lungs. A disadvantage is radiation; however, given its short examination time, CT can be useful in patients who cannot tolerate a lengthy MRI examination, and it avoids the need for sedation. It is the recommended confirmatory modality for PAVMs after positive findings are seen at screening transthoracic echocardiography in patients with known or suspected HHT (11). Guidelines recommend noncontrast thin-section CT for confirmation of diagnosis, which requires visualization of a feeding artery and draining vein. However, dedicated contrast-enhanced CT pulmonary angiography is preferred by some radiologists and has the advantage of delineation of architecture for pretreatment planning, as well as exclusion of other entities that can mimic AVM (16). In these cases, a wet-to-wet connection is mandatory to avoid air embolism. In soft-tissue venous malformations, CT can demonstrate phleboliths and osseous involvement, although the preferred modality is MRI given its superior contrast resolution (5). Some studies have shown the potential role of low-dose time-resolved CT angiography using dual-source CT as an alternative imaging modality for venous malformations in the pediatric population (17). In vascular tumors, especially malignant tumors, CT can demonstrate the extent as well as metastatic spread.

Conventional Angiography

Conventional angiography is typically not the initial test because of its invasiveness and ionizing radiation. The main role is in treatment (ie, embolization) (18).

Molecular Imaging

Nuclear medicine is less commonly used but may be helpful in some scenarios. For example, PET/CT can aid in diagnosis and monitoring of vascular tumors (7). In addition, new tracers are showing promise in imaging AVMs by depicting angiogenesis and allowing identification of treatment targets (18).

Imaging Spectrum of Vascular Malformations

This article focuses on commonly encountered cardiothoracic vascular anomalies, where the radiologist can play an important role in management. Rarely encountered anomalies with nonspecific imaging findings have not been detailed in this review.

The spectrum of simple vascular malformations is provided in Table 2. The following discussion focuses on high-flow lesions with an arterial component (AVM, AVF) and slow-flow lesions, such as venous and lymphatic malformations in the thorax. These anomalies have unique imaging features that can clue in the radiologist. Some simple vascular malformations, such as capillary malformations, present with a "port wine stain" at physical examination (5) and are usually diagnosed clinically.

High-Flow Lesions

AVMs and AVFs are high-flow lesions connecting arteries to veins, bypassing the normal capillary bed (16,19,20). AVMs are typically congenital, demonstrating a tangle of vessels (ie, nidus) (Fig 1), whereas AVFs are usually acquired (eg, posttraumatic) and consist of a direct artery-to-vein communication without an intervening nidus (21) (Fig 2).

These high-flow vascular malformations can occur in the chest wall, mediastinum (22), or deep structures, especially the lungs in the context of HHT (20). HHT accounts for 80%–90% of PAVMs, with the lungs being the most common site of visceral AVMs. Although often asymptomatic, right-to-left shunt in PAVM can lead to dyspnea, paradoxical emboli, and brain abscess (20). Untreated PAVMs are likely to increase in size over time, and sudden accelerated growth may sometimes result from trauma or hormonal influence (especially during puberty or pregnancy).

Table 1: Broad Overview of International Society for the Study of Vascular Anomalies Classification Updated in 2018

Vascular Malformations	Vascular Tumors
Features	
Nonneoplastic structural abnormalities	Neoplastic
Do not show increased endothelial cell turnover or mitosis	Show increased endothelial cell turnover or mitosis
Growth is usually proportionate to somatic growth	Growth is independent of somatic growth
Never spontaneously regress	Can spontaneously regress (eg, infantile hemangiomas)
Classification	
Simple	Benign
Combined	Locally aggressive
Malformations of major named vessels	Malignant
Malformations associated with other anomalies	Other

Note.—Adapted, under a CC BY 4.0 license, from reference 1 *(issva.org/classification)*.

Table 2: Key Characteristics of Simple Vascular Malformations in the Chest by Flow State

High flow
AVM and AVF
Direct communication between artery and vein bypassing capillary bed
AVM
Consists of dilated feeding artery, nidus, and dilated draining vein
Usually congenital
AVF
Direct communication between dilated artery and vein without nidus
Usually acquired
Low flow
Venous malformations
Most common vascular anomaly
Usually present early in life
Do not spontaneously regress
Multispatial and heterogeneous
MRI: given slow-flow anomaly, high signal at T2-weighted imaging and lack of flow voids
Various enhancement patterns depending on acquisition timing (slow to rapid and homogeneous to heterogeneous)
Dynamic time-resolved MR angiography: absence of arterial enhancement with gradual persistent enhancement at delayed imaging
US: monophasic venous flow or no flow
Phleboliths in 40% of cases
Lymphatic malformations
Typically present in childhood
Transspatial, involving multiple tissue planes
Macrocystic type: composed of larger cysts
Microcystic type: composed of tiny cysts
Mixed type: features overlap those of microcystic and macrocystic types
Capillary malformations
Usually clinically evident as “port wine” stain
Imaging is not needed for diagnosis

Note.—AVF = arteriovenous fistula, AVM = arteriovenous malformation.

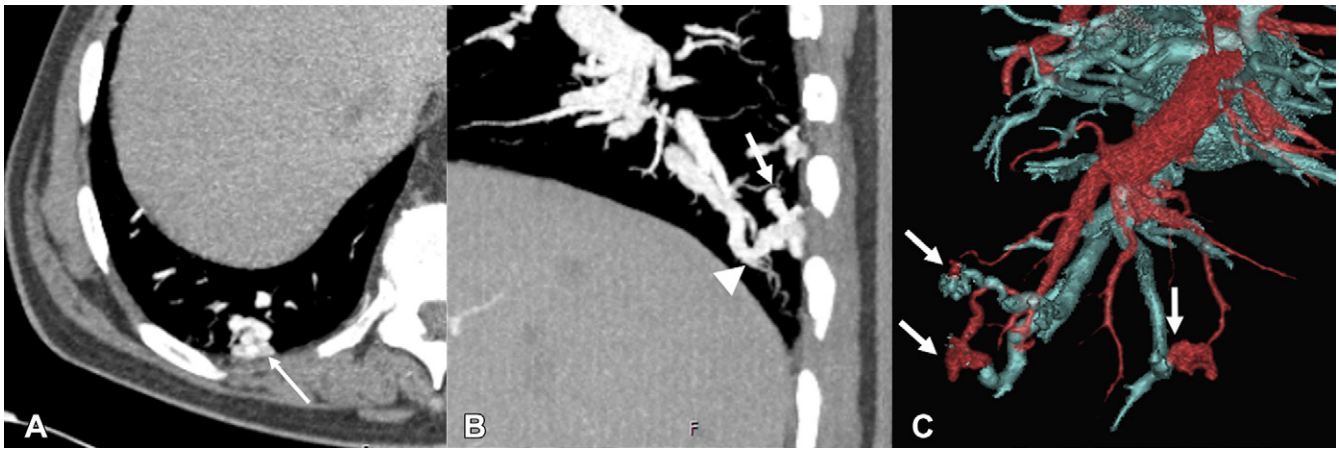

Figure 1: Images in a 76-year-old-male patient with hereditary hemorrhagic telangiectasia and multiple pulmonary arteriovenous malformations. **(A)** Axial contrast-enhanced CT scan shows a tangle of vessels (arrow). **(B)** Sagittal contrast-enhanced chest CT scan shows a tangle of vessels with a feeding artery (arrow) and a draining vein (arrowhead). **(C)** Three-dimensional volume-rendered reconstruction demonstrates multiple pulmonary arteriovenous malformations (arrows), with arteries depicted in red and veins in blue.

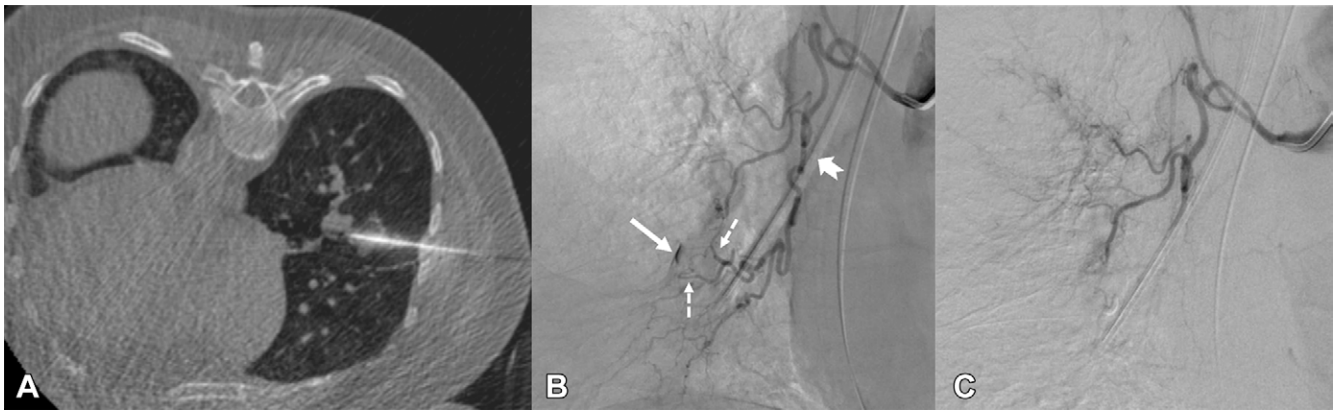

Figure 2: Images in a 58-year-old female patient with an iatrogenic arteriovenous fistula (AVF) after percutaneous biopsy of a pulmonary nodule. **(A)** CT image shows the path of the biopsy needle in the right lower lobe targeting the nodule, with mild perilesional hemorrhage. This was followed by hemoptysis and cough with desaturation to 88% with the patient breathing room air. At bronchoscopy, a clot occluding the bronchus intermedius was observed; it was removed, and an endobronchial blocker was left deflated at the level of the opening of right lower lobe bronchus. **(B)** Digital subtraction angiography was subsequently performed and showed an AVF between the right bronchial artery branches (dashed arrows), with early enhancement of a small pulmonary venous branch (solid arrow). Note the deflated endobronchial blocker (notched arrow). **(C)** After embolization with a gelatin compressed sponge, the abnormal flow and venous enhancement were no longer visualized. The patient was extubated with no further hemoptysis.

Imaging features consist of dilated feeding arteries and draining veins, with nidus (AVM) or without nidus (AVF), and no discernible soft-tissue component. For superficial lesions, Doppler US can show low-resistance, monophasic arterial flow within feeding arteries and pulsatile high flow within draining veins. CT and MRI show dilatation of feeding arteries and draining veins with early vein opacification, consistent with shunting (5) (Fig 1). The initial telangiectatic stage of PAVM may be observed as a solid or ground-glass lung nodule at CT that shows progressive pulmonary venous enlargement (microscopic arteriovenous communication) and finally evolves to the typical AVM with a discrete nidus (23). A comprehensive imaging evaluation for proper treatment planning (24) includes determining whether there are single or multiple AVMs (multiple AVMs indicate underlying HHT) and determining the number and caliber of feeding arteries.

Treatment options include transcatheter or direct percutaneous embolization and alcohol sclerotherapy. Embolization of PAVM is aimed at occluding the feeding arteries and nidus and is usually indicated if the feeding artery (measured 2–3 mm proximal to the nidus) is greater than 2 mm (16) (24).

For imaging surveillance of treated PAVMs, CT is helpful to monitor regression or reperfusion (24,25) and can be performed at 6 months to 1 year (11). Echocardiography is not useful because findings remain positive in almost 90% of patients after embolization (11). Studies show that 96% of treated PAVMs become undetectable or reduced in size (24). Shrinkage of the aneurysmal sac and draining veins are important imaging findings indicating treatment success. CT evaluation may be rendered difficult by substantial beam-hardening artifact from coils; use of metal artifact reduction algorithms may be helpful in these cases (26).

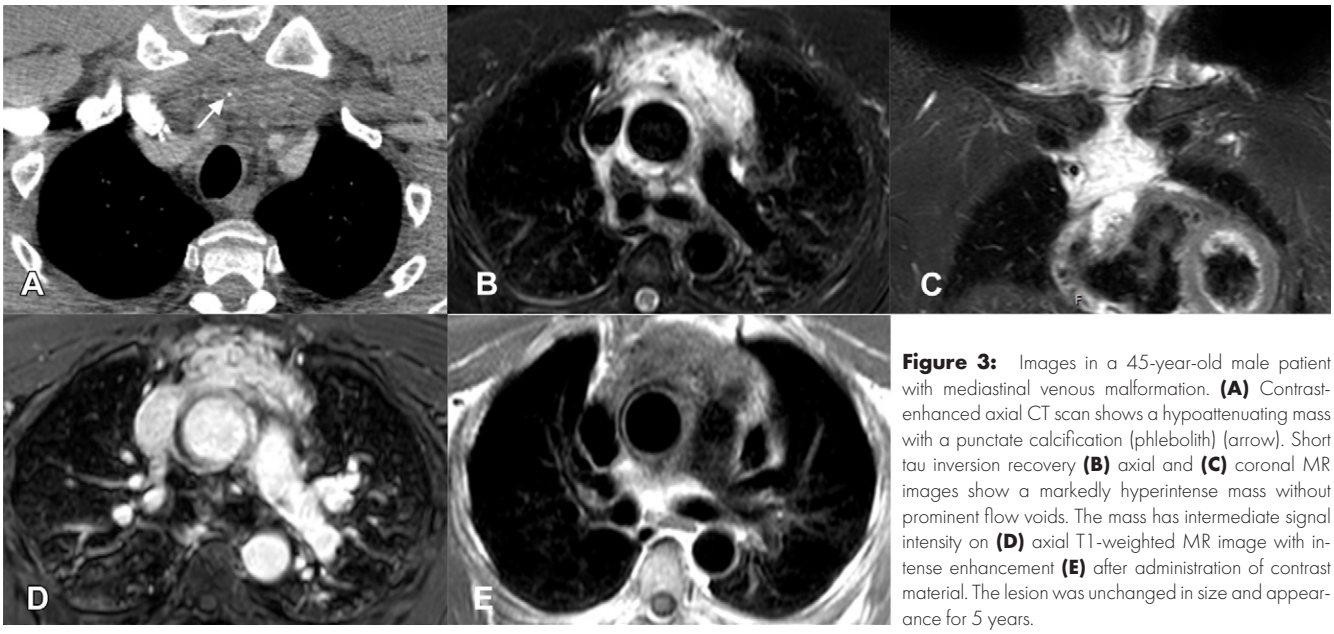

Figure 3: Images in a 45-year-old male patient with mediastinal venous malformation. **(A)** Contrast-enhanced axial CT scan shows a hypoattenuating mass with a punctate calcification (phlebolith) (arrow). Short tau inversion recovery **(B)** axial and **(C)** coronal MR images show a markedly hyperintense mass without prominent flow voids. The mass has intermediate signal intensity on **(D)** axial T1-weighted MR image with intense enhancement **(E)** after administration of contrast material. The lesion was unchanged in size and appearance for 5 years.

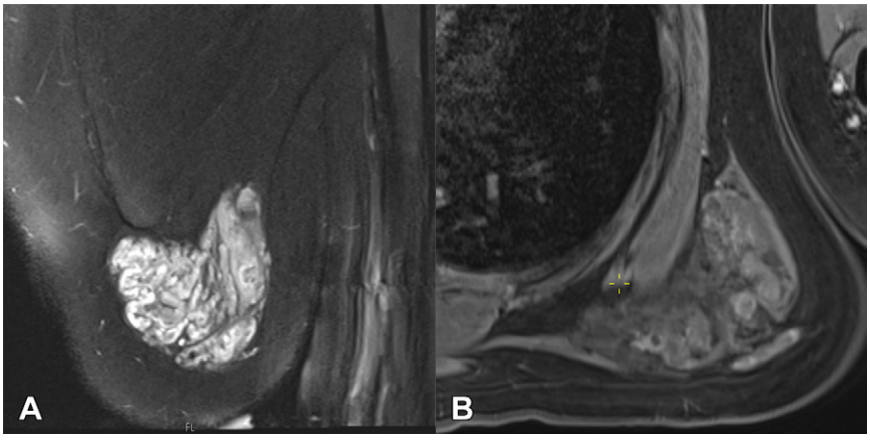

Figure 4: Images in a 43-year-old female patient who presented with a left upper back mass (venous malformation) causing substantial pain. **(A)** Oblique coronal fat-saturated T2-weighted MR image shows marked hyperintense mass with tubular structures. **(B)** Postcontrast T1-weighted MR image shows heterogeneous enhancement within the mass.

Slow-Flow Lesions

Venous malformations (VMs) are the most common vascular anomaly, with an incidence of one to two in 10 000 (12). Although typically diagnosed in childhood (5,12), these malformations may escape detection until adulthood. VMs grow in concert with the body and do not spontaneously regress (27). Because of stagnant blood flow, they can thrombose, causing pain, swelling, and skin changes (12). VMs are classified into four subtypes: type I, isolated without venous connection; type II, draining into normal veins (3); type III, draining into dysplastic veins; and type IV, consisting of venous ectasia (28).

Doppler US and MRI are key imaging methods to characterize and diagnose VMs; CT is usually not the first-line modality but can demonstrate phelobliths (Fig 3). At imaging, VMs can be multispatial and heterogeneous (12). Phleboliths, a characteristic feature, are observed in 40% of cases (5,29) and appear as acoustic shadowing at US, signal void at MRI, and calcification at CT. VMs appear as multiple tubular structures with monophasic venous flow at Doppler US, although 16% have little or no demonstrable flow (16). At MRI, VMs demonstrate marked T2 hyperintensity because of slow flow; hence, T2-weighted imaging is excellent in determining lesion extent (Fig 4). Unlike in hemangiomas and AVMs, flow voids are not a major feature in VMs due to slow flow, but occasional dysplastic draining or ectatic veins may be visualized (30). After administration of contrast material, enhancement patterns range from slow to rapid and homogeneous to heterogeneous, depending on acquisition timing. Dynamic time-resolved MR angiography can be helpful in showing absence of arterial enhancement, with gradual persistent enhancement at delayed imaging (28). Depending on the size and location, no treatment may be needed. If the patient is symptomatic, options include surgery, sclerotherapy, and ablation.

Lymphatic malformations (LMs) are low-flow vascular malformations that are typically identified by age 2 years in 80%–90% cases (31) but sometimes may present later in life. They do not communicate with normal lymphatic structures and are mostly seen in subcutaneous tissue of the head and neck (70%–80%); they can also extend to the thorax (31,32). LMs are transspatial, disregarding anatomic and fascial boundaries, and thus involve multiple tissue planes with or without mass effect on adjacent structures. LMs can lead to osseous hypertrophy and potential limb-length discrepancy (31,32). Diagnosis is typically

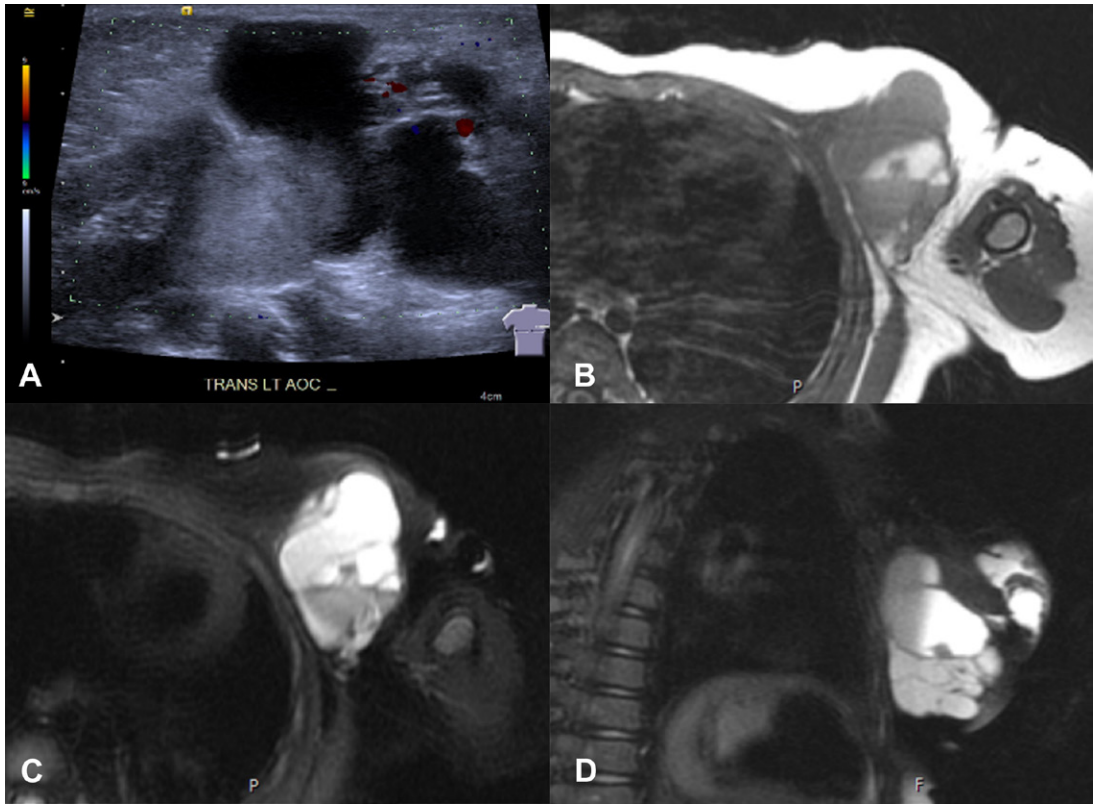

Figure 5: Images in a 4-year-old male patient with a palpable mass in the left axillary area (macrocystic lymphatic malformation). **(A)** Color Doppler US image shows a left subpectoral anechoic multilobulated mass with thin septations and without discernible flow. **(B)** Axial T1-weighted, **(C)** axial T2-weighted, and **(D)** coronal T2-weighted MR images show the cystic nature with hypointensity at T1-weighted imaging, hyperintensity at T2-weighted imaging, and fluid-fluid level. These are findings typical of macrocystic lymphatic malformation.

clinical for superficial lesions, although deep-seated lesions may be discoverable only at imaging. Imaging is used to confirm diagnosis, evaluate the extent of disease, and plan therapy.

LMs are subdivided into macrocystic, microcystic, and mixed types (31,32) on the basis of cyst dimensions (33). Macrocystic LMs (>2 cm) are multicystic, often with fluid-fluid levels (Fig 5) (28,32). In comparison, microcystic LMs (<2 cm) appear as an ill-defined echogenic mass with or without identifiable discrete tiny cysts at US. At MRI, microcystic LMs appear as T1 hypointense and T2 hyperintense lesions, with small cysts (28). Imaging features of mixed type overlap those of microcystic and macrocystic types.

In LMs, mild enhancement can be observed along the walls or septae (34). Calcifications are uncommon in pure LMs but can be observed in combined malformation (eg, lymphatic-venous malformation) (5). CT may show macrocystic and microcystic LMs as fluid-filled hypoattenuating masses with slight wall enhancement at the delayed phase (2) and is also crucial in determining intrathoracic extension (35).

Treatment options include sclerotherapy, laser therapy, and resection for macrocystic LMs, and percutaneous drainage, resection, or sometimes interstitial bleomycin for microcystic LMs (2).

Vascular Malformation Syndromes

Vascular malformations can occur sporadically or as part of a syndrome. The ISSVA lists various syndromes and underlying genetic causes (1). A comprehensive review of syndromes (often with extrathoracic manifestations) is outside the scope of this article, which focuses on lesions relevant to the cardiothoracic radiologist. In the following section we briefly describe some relevant syndromes.

Syndromes associated with simple vascular malformations include HHT (associated with PAVMs), blue rubber bleb nevus syndrome (VMs involving skin, gastrointestinal, and musculoskeletal systems), and those associated with LMs, such as generalized lymphatic anomaly and Gorham–Stout syndrome (32). Generalized lymphatic anomaly and Gorham–Stout syndrome share features such as chylous effusions, ascites, LM, and bone lesions. However, bone lesions in Gorham–Stout syndrome are characteristically progressively lytic with cortical bone resorption, unlike generalized lymphatic anomaly.

Various other syndromes are categorized as vascular malformations associated with other anomalies. Examples include those that are part of *PIK3CA*-related overgrowth spectrum (ie, Klippel–Trenaunay syndrome, CLOVES [congenital lipomatous overgrowth, vascular malformations, epidermal nevi, spinal/skeletal anomalies and/or scoliosis] syndrome, and CLAPO [capillary malformations of the lower lip, lymphatic malformations of the face and neck, asymmetry of the face and limbs, and partial or generalized overgrowth] syndrome) and others (such as Sturge–Weber syndrome and Maffucci syndrome). Among *PIK3CA*-related overgrowth

Table 3: Key Characteristics of Vascular Tumors in the Chest

Benign
Infantile hemangioma
Not present at birth (GLUT-1 positive)
Triphasic growth pattern
Imaging appearance (rarely needed):
US: Hyper- or hypoechoic lesions with hypervascularity
MRI: T2 hyperintense enhancing lesions with prominent flow voids and avid enhancement
Congenital hemangioma
Present at birth (GLUT-1 negative)
Classified by rate of involution
Imaging features same as infantile hemangioma
Locally aggressive or borderline
Kaposiform hemangioendothelioma
Usually present within 1st year after birth
Associated with Kasabach–Merritt phenomenon
Imaging: Heterogeneous locally invasive mass with enhancement
Kaposi sarcoma
Subtypes: classic, iatrogenic (related to organ transplant), AIDS-related, and African (endemic)
CT findings: flame-shaped lung nodules, halo sign, thickened bronchovascular structures, pleural effusions, lytic osseous lesions
Malignant
Epithelioid hemangioendothelioma
Lungs are third most common site
Four imaging patterns:
Multinodular
Reticulonodular
Parenchymal tumor with pleural invasion
Diffuse pleural thickening
Angiosarcoma
Poor prognosis
Usually occurs in 6th or 7th decade of life
Aggressive mass with heterogeneous appearance at CT and MRI, along with enhancement

Note.—GLUT-1 = glucose transporter 1.

spectrum, Klippel–Trenaunay syndrome and CLOVES can have thoracic manifestations.

Klippel–Trenaunay syndrome is characterized by asymmetric limb hypertrophy, a cutaneous port wine stain (capillary malformation), congenital lower extremity varicose veins as well as abnormalities of deep veins predisposing to deep-vein thrombosis and pulmonary embolism (36). In addition to the capillary malformation, lymphatic and venous malformations can also occur (37).

CLOVES syndrome is associated with congenital lipomatous overgrowth (may involve the thorax and abdomen) and vascular malformations, such as LMs, VMs, and capillary malformations (35), along with spinal anomalies or scoliosis (38).

Imaging Spectrum of Vascular Tumors

The spectrum of vascular tumors is provided in Table 3. The following discussion focuses on hemangiomas (infantile and congenital), kaposiform hemangioendothelioma, Kaposi sarcoma, epithelioid hemangioendotheliomas, and angiosarcomas. Entities such as pyogenic granulomas and other less common hemangioendotheliomas (eg, retiform) are rare and their imaging appearances are not well described; hence, these entities are not discussed in this review.

Benign Vascular Tumors

Hemangiomas are divided into infantile and congenital hemangioma and result from dysregulation of both vasculogenesis and angiogenesis stimulated by overexpression of vascular endothelial growth factor (39). Endothelial cells of infantile hemangiomas express the immunologic marker glucose transporter 1 (GLUT-1), in contrast to congenital hemangiomas, which are GLUT-1 negative. Typically, infantile hemangiomas are absent at birth and demonstrate a triphasic growth pattern of rapid initial enlargement during infancy, stabilization and

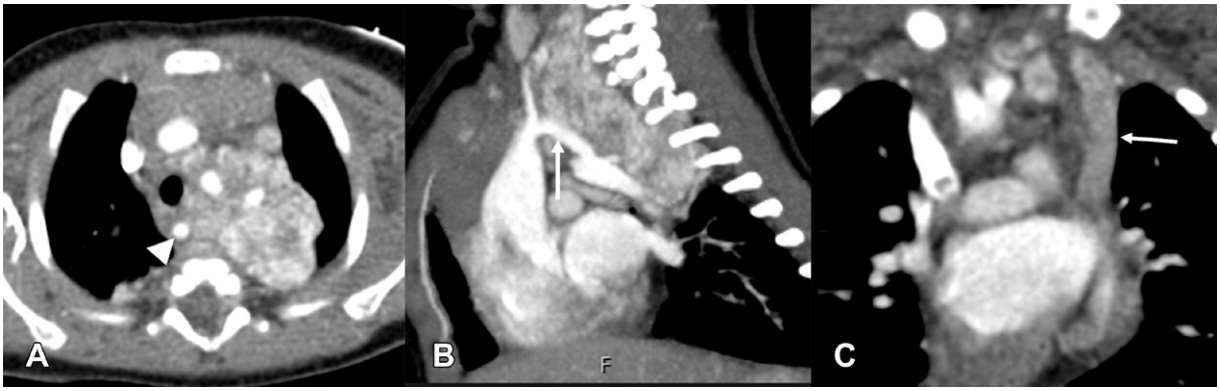

Figure 6: Images in a 6-year-old female patient with PHACE syndrome, extensive hemangiomas in the skin, chest, and abdomen, and hypoplastic aortic arch with gradient of 60 mm Hg at echocardiography. CT was performed to assess the mediastinal hemangioma and relation to aortic arch for preoperative planning. **(A)** Axial and **(B)** sagittal contrast-enhanced CT images show a heterogeneously enhancing mass involving the mediastinum, consistent with hemangioma closely related to and enveloping the hypoplastic aortic arch (arrow, **B**). The patient had a left arch with aberrant right subclavian artery (arrowhead, **A**) and **(C)** a persistent left superior vena cava draining to the coronary sinus (arrow) on the coronal image. Given the close relation to hemangiomas, the surgical plan was to perform an interposition graft or patch angioplasty from distal ascending to proximal descending aorta. The arch was successfully dissected from the hemangiomas, and patch angioplasty was performed. PHACE = posterior fossa malformations, hemangiomas, arterial anomalies, cardiac abnormalities, and eye anomalies.

regression in the following years, and then complete involution (7,39). Diagnosis is clinical; imaging is used only in cases of diagnostic uncertainty and to determine associated findings, plan treatment, and evaluate complications. Infantile hemangiomas may be associated with other anomalies in PHACE (posterior fossa malformations, hemangiomas, arterial anomalies, cardiac abnormalities, and eye anomalies) syndrome (Fig 6). The term PHACES is used if there is sternal cleft or supraumbilical raphe.

At US, infantile hemangiomas are hyper- or hypoechoic lesions with hypervascularity at Doppler imaging. At MRI, they are T2 hyperintense enhancing lesions with prominent flow voids, suggesting serpiginous vessels during their proliferation period (Fig 7) (5). Involuting infantile hemangiomas demonstrate fibrofatty infiltration with T1 hyperintense foci and decreased contrast enhancement.

Congenital hemangiomas are rare and fully developed at birth. Imaging findings of congenital hemangiomas are similar to those seen with infantile hemangiomas. They are classified by their rate of involution into rapidly involuting congenital hemangiomas, partially involuting congenital hemangiomas, and noninvoluting capillary hemangiomas, with involuting hemangiomas having decreased vascularity and enhancement (5).

The term *hemangioma* is often erroneously used for lesions more aptly termed VMs. A true hemangioma is a neoplasm with flow voids, whereas a VM is a malformation that shows phleboliths and lacks flow voids (from slow flow).

Congenital hemangiomas may require therapy because of complications, such as high-output cardiac failure or thrombocytopenia.

Locally Aggressive Vascular Tumors

Kaposiform hemangioendothelioma.— Kaposiform hemangioendothelioma is the most common locally aggressive tumor, with an incidence of one in 100 000 000 (5), which usually presents within the 1st year after birth and portends a poor prognosis (5). Pathologically, these are GLUT-1 negative and composed of vascular and lymphatic components, with infiltrative spindle endothelial nodules (40). Thrombocytopenia, pain, and diffuse intravascular coagulation (Kasabach–Merritt phenomenon) can occur (7,41). MRI findings include a locally aggressive mass with heterogeneous T2 hyperintensity, hemosiderin deposits, and notable enhancement (Fig 8). There may also be adjacent bone involvement (5,42). The presence of a hypervascular infiltrative mass, accompanied by Kasabach–Merritt phenomenon and reticular lymphedema with speckled hypointense signal at T2-weighted imaging, especially in the pediatric population, is highly suggestive of this entity (40). Treatment includes medical therapy along with chemotherapeutic agents (43,44).

Kaposi sarcoma.— Kaposi sarcoma is a mesenchymal tumor arising from lymphatic endothelial cells (5) with four subtypes: classic, iatrogenic (related to organ transplantation), AIDS-related, and African (endemic). Human herpesvirus type 8 plays an important role in pathogenesis of all subtypes, especially in the immunocompromised setting (5,7). Cutaneous and mucosal involvement is common, but Kaposi sarcoma has the potential to involve the lungs, pleura, tracheobronchial tree, or chest wall (45). Pulmonary involvement can cause dyspnea, dry cough, and life-threatening hemoptysis (45). At CT, common features of intrathoracic Kaposi sarcoma are bilateral flame-shaped pulmonary mass or nodules (occasionally larger asymmetrically distributed masses may be observed), halo sign (ground-glass surrounding solid nodules), thickened bronchovascular structures, and pleural effusions (Fig 9) (45,46). These imaging features can overlap with infections, particularly fungal (47). Lytic osseous lesions and soft-tissue masses may also be encountered in thoracic wall Kaposi sarcoma (47).

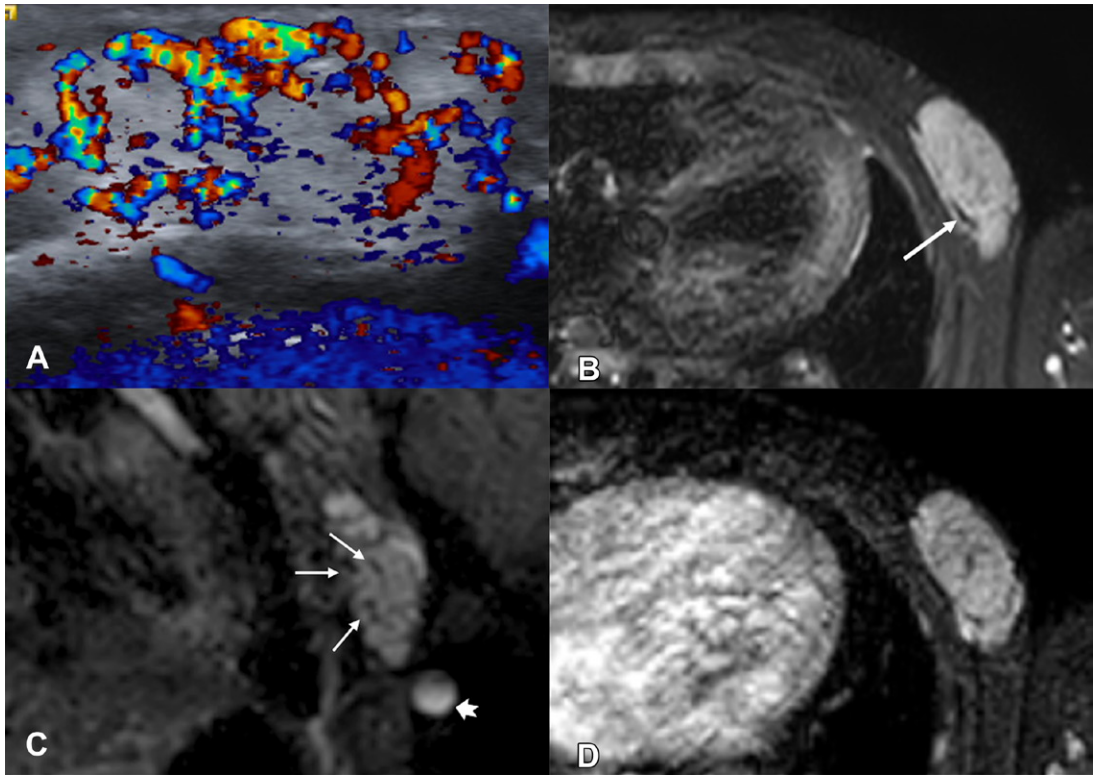

Figure 7: Images in a 6-month-old male patient with infantile hemangioma presenting as a palpable lump in the left chest wall with bluish tint. According to the mother, the mass increased in size over 1 month. **(A)** Color Doppler US image shows a hypervascular hyperechoic mass in the left chest wall. **(B)** Axial and **(C)** coronal fat-saturated T2-weighted MR images show a T2 hyperintense mass lesion with prominent flow voids (arrows) corresponding to the lump, indicated by the skin marker (notched arrow, **C**). **(D)** Contrast-enhanced T1-weighted MR image shows the intensely enhancing mass.

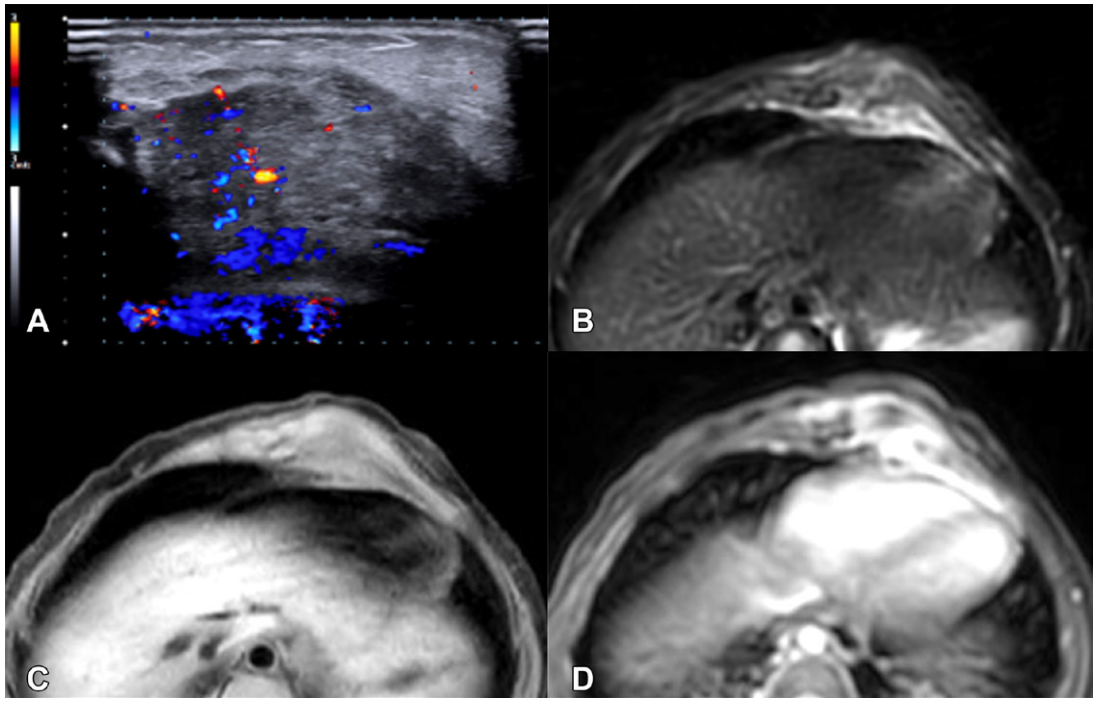

Figure 8: Images in an 8-month-old male patient with a left chest wall mass. Lesion biopsy indicated kaposiform hemangioendothelioma. **(A)** Color Doppler US image shows a heterogeneously echogenic mass with mild vascularity. **(B)** Fat-suppressed T2-weighted MR image shows a heterogeneous mass with areas of hypo- and hyperintensity in the chest wall involving adjacent bones. Fat-suppressed T1-weighted **(C)** pre- and **(D)** postcontrast MR images show heterogeneous enhancement.

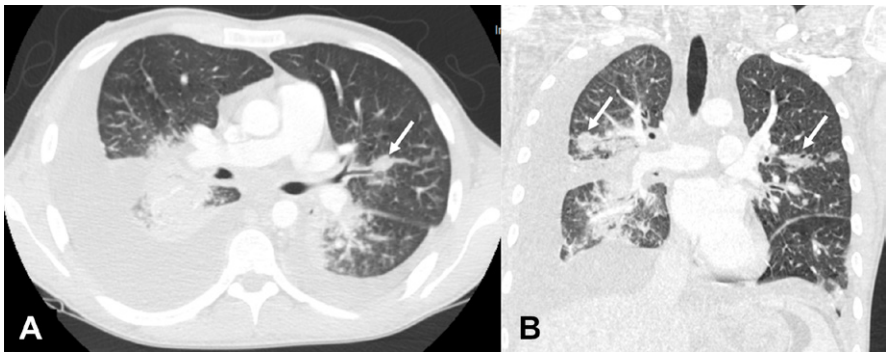

Figure 9: Images in a 24-year-old HIV-positive male patient with hemoptysis and biopsy-confirmed Kaposi sarcoma. **(A)** Axial and **(B)** coronal contrast-enhanced CT images (lung window) show flame-shaped lung nodules (arrows).

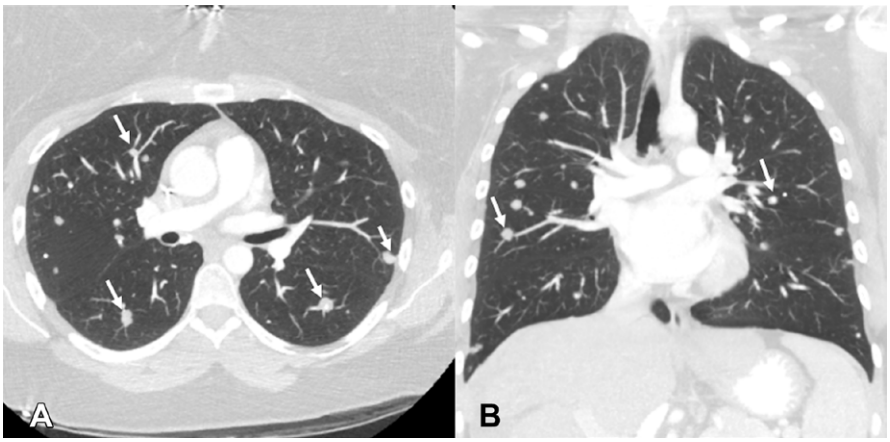

Figure 10: Images in a 26-year-old female patient who presented with shortness of breath and biopsy-proven hemangioendothelioma. **(A)** Axial and **(B)** coronal contrast-enhanced chest CT images show multiple noncalcified solid nodules (arrows), with several observed along the bronchovascular structures.

Malignant Vascular Tumors

Epithelioid hemangioendotheliomas are rare (<1% of all vascular malignancies) vascular neoplasms originating from vascular endothelial or pre-endothelial cells (5,7,48). The lungs are the third most common site of involvement (12%), after the liver (21% of patients) and bone (14%) (48). They show multiplicity as well as potential to metastasize. When the tumor is first identified as involving multiple sites in the body, it is difficult to determine whether the lesions represent multicentric tumors or metastases from a single lesion. CT features of pulmonary epithelioid hemangioendothelioma can show four imaging patterns: multinodular, reticulonodular, parenchymal tumor with pleural invasion, and diffuse pleural thickening (48–50). The most common multinodular pattern is characterized by multiple discrete nodules (punctate to 2 cm) (Fig 10) predominantly along bronchovascular structures and has the best prognosis (48,50). Unlike hematogenous metastases from primary tumors, these lesions demonstrate relatively little growth over serial examinations. Tumor calcification and cavitation are rare. The reticulonodular pattern is characterized by interlobular septal thickening, nodules, and ground-glass opacities (50), with the histopathologic correlate of infiltrating nodular proliferation of neoplastic cells along small blood and lymphatic vessels (50). The parenchymal tumor with pleural invasion pattern is less common and associated with the worst prognosis; it appears as solitary or multiple lung masses or nodules extending to the adjacent pleura, often with an effusion (48). The diffuse pleural thickening pattern is uncommon and is characterized by smooth or nodular pleural thickening, which can involve the fissures. This pattern is often confused with pleural mesothelioma or pleural metastases (48, 51), and diagnosis is based on pathologic findings.

Angiosarcoma

Angiosarcomas are malignant tumors arising from vascular endothelial cells and occur in the 6th to 7th decade of life. Known risk factors include chronic lymphedema; radiation therapy; various exogenous toxins (such as arsenic or vinyl chloride); and genetic predisposition in neurofibromatosis type 1, Maffucci syndrome, or Klippel–Trenaunay syndrome (7). Chemotherapy is usually ineffective, and prognosis is poor (52). In the thorax, angiosarcomas can involve the major vessels (eg, pulmonary artery, aorta), heart, and chest wall and/or breast (53,54).

Pulmonary artery angiosarcoma is observed as a filling defect within the central pulmonary arteries, mimicking pulmonary embolism (Fig 11). Extravascular extension, metastases, and enhancement of the filling defect are key features to differentiate this lesion from emboli, although enhancement may be difficult to identify at CT (55). PET can show high metabolic activity of the filling defect, which is useful in distinguishing angiosarcoma from acute or chronic pulmonary emboli (56). Although some uptake can be observed in bland thrombi using PET, a study showed that with use of a maximum standardized uptake value cutoff of 3.3, the sensitivity, specificity, and accuracy of PET were 98.4%, 96.8%, and 97.8%, respectively (57). At MRI, angiosarcomas are usually T1 isointense, T2 hyperintense, and heterogeneously enhancing.

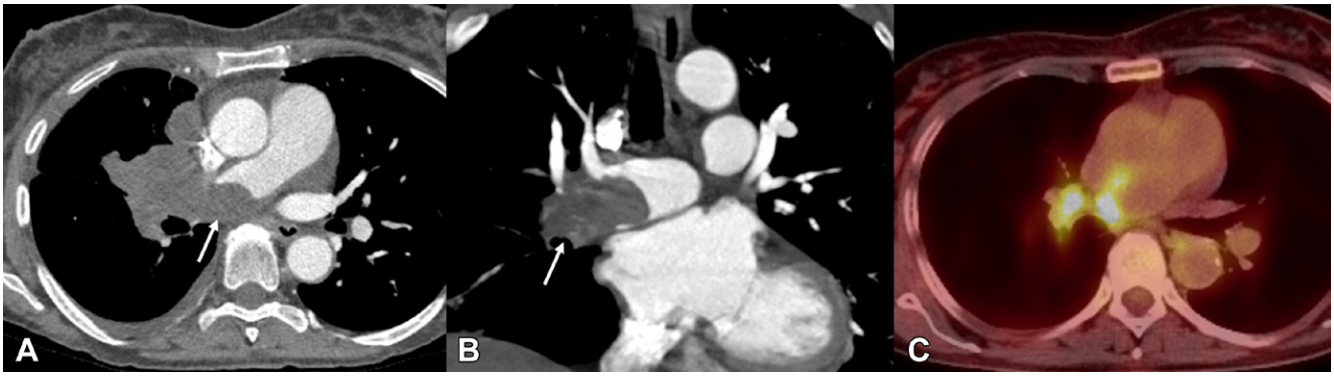

Figure 11: Images in a 74-year-old female patient with shortness of breath and biopsy-proven pulmonary artery angiosarcoma. **(A)** Axial and **(B)** coronal contrast-enhanced CT images show large occlusive filling defect in the main right pulmonary artery with a lobulated appearance and extension to adjacent structures (arrow, **A**). The filling defect shows heterogeneity with mild enhancement (arrow, **B**). **(C)** Fluorodeoxyglucose (FDG) PET/CT image shows corresponding FDG avidity, suggesting a neoplastic process rather than pulmonary embolism.

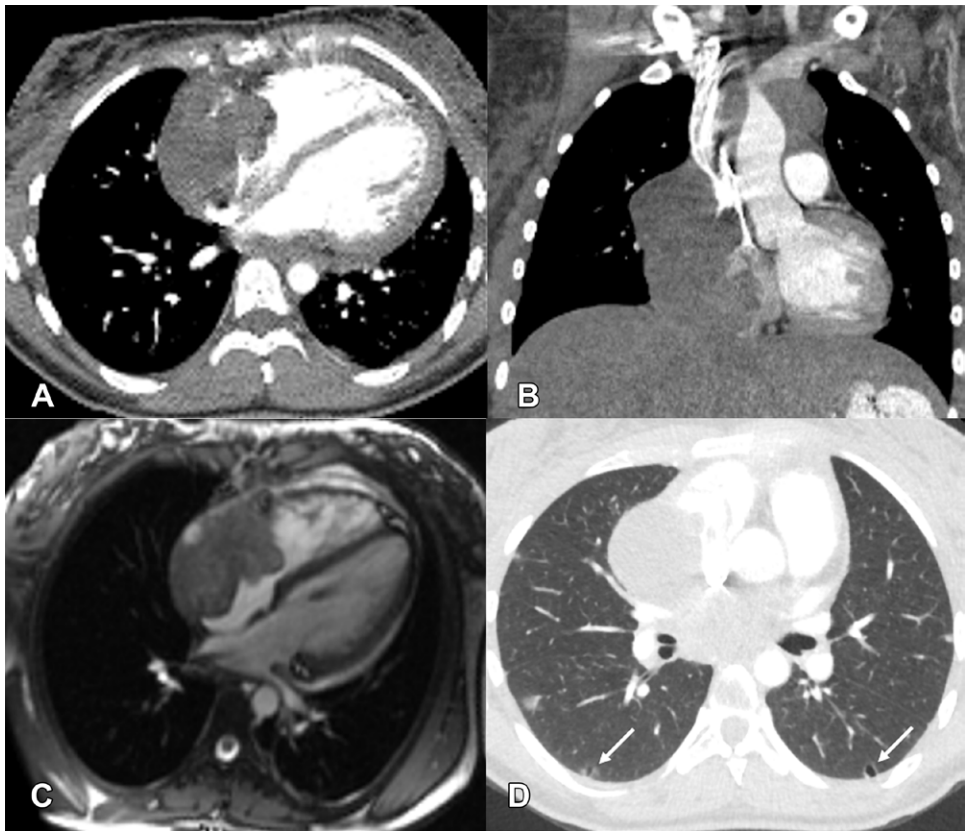

Figure 12: Images in a 28-year-old female patient with cardiac angiosarcoma. **(A)** Axial and **(B)** coronal contrast-enhanced CT images show a lobulated infiltrative mass centered in the lateral wall of the right atrium extending into the pericardium and right atrioventricular groove. **(C)** Still frame from steady-state free precession MRI shows that the mass spares the interatrial septum and is heterogeneous. **(D)** Axial CT lung windows show multiple cavitary nodules (arrows), suggesting metastatic disease.

Cardiac angiosarcoma usually occurs in the right atrial lateral wall and, given its infiltrative nature, can involve adjacent structures (58). Contrast-enhanced CT shows a well-defined, highly vascular mass. At MRI, the mass is often heterogeneous from hemorrhage and necrosis, T1 isointense, T2 hyperintense, and irregularly enhancing with internal flow voids and characteristic "cauliflower" configuration (Fig 12) (55,59). A differential consideration for a primary tumor in this region includes cardiac lymphoma. Although lymphomas are infiltrative and can surround the right coronary artery, the vessel floating sign (coronary artery encased by mass but without vascular involvement or narrowing) is a characteristic feature of malignant lymphoma, differentiating it from angiosarcoma (60).

In the chest wall, angiosarcoma can involve the breast (54). Primary breast angiosarcoma occurs without underlying causes, whereas secondary breast angiosarcoma is more common and

usually associated with lymphedema after radiation treatment. MRI shows a mass with T1 hypointensity, T2 hyperintensity, necrotic and cystic components with rapid enhancement, and various washout patterns at dynamic postcontrast imaging (54). Cutaneous angiosarcoma can occur in the thorax but is much more common in the scalp.

Conclusion

Vascular malformations and tumors in the chest can be misdiagnosed because of unfamiliarity with imaging appearance and use of inaccurate archaic terms in clinical practice. To understand the spectrum and relevance of these lesions, cardiothoracic radiologists should be familiar with the ISSVA classification. Increased knowledge of cardiothoracic vascular lesions and their typical imaging features will aid in making accurate diagnoses.

Disclosures of conflicts of interest: Y.O. No relevant relationships. **E.L.** No relevant relationships. **E.S.** No relevant relationships. **P.A.** ACR FCRI grant (co- principal investigator); Spiromics Heart Failure Substudy (co-investigator); *Radiology: Cardiothoracic Imaging* editorial board member; support for travel for RSNA GLC program and ABR Cardiac Core Committee; Editor-in-Chief for *Seminars in Roentgenology*; vice president of NASCI.

References

1. ISSVA classification of vascular anomalies. International Society for the Study of Vascular Anomalies. https://www.issva.org/UserFiles/file/ISSVA-Classification-2018.pdf. Published 2018. Accessed December 9, 2022.
2. Wang MX, Kamel S, Elsayes KM, et al. Vascular anomaly syndromes in the ISSVA classification system: imaging findings and role of interventional radiology in management. RadioGraphics 2022;42(6):1598–1620.
3. Monroe EJ. Brief description of ISSVA classification for radiologists. Tech Vasc Interv Radiol 2019;22(4):100628.
4. Wassef M, Blei F, Adams D, et al; ISSVA Board and Scientific Committee. Vascular anomalies classification: recommendations from the International Society for the Study of Vascular Anomalies. Pediatrics 2015;136(1):e203–e214.
5. Brahmbhatt AN, Skalski KA, Bhatt AA. Vascular lesions of the head and neck: an update on classification and imaging review. Insights Imaging 2020;11(1):19.
6. Antonescu C. Malignant vascular tumors--an update. Mod Pathol 2014;27(Suppl 1):S30–S38.
7. Wildgruber M, Sadick M, Müller-Wille R, Wohlgemuth WA. Vascular tumors in infants and adolescents. Insights Imaging 2019;10(1):30.
8. Hassanein AH, Mulliken JB, Fishman SJ, Greene AK. Evaluation of terminology for vascular anomalies in current literature. Plast Reconstr Surg 2011;127(1):347–351.
9. Rohatgi S, Howard SA, Tirumani SH, Ramaiya NH, Krajewski KM. Multimodality imaging of tumour thrombus. Can Assoc Radiol J 2015;66(2):121–129.
10. Esposito F, Ferrara D, Di Serafino M, et al. Classification and ultrasound findings of vascular anomalies in pediatric age: the essential. J Ultrasound 2019;22(1):13–25.
11. Faughnan ME, Palda VA, Garcia-Tsao G, et al; HHT Foundation International - Guidelines Working Group. International guidelines for the diagnosis and management of hereditary haemorrhagic telangiectasia. J Med Genet 2011;48(2):73–87.
12. Behravesh S, Yakes W, Gupta N, et al. Venous malformations: clinical diagnosis and treatment. Cardiovasc Diagn Ther 2016;6(6):557–569.
13. Flors L, Leiva-Salinas C, Maged IM, et al. MR imaging of soft-tissue vascular malformations: diagnosis, classification, and therapy follow-up. RadioGraphics 2011;31(5):1321–1340; discussion 1340–1341.
14. Mamlouk MD, Nicholson AD, Cooke DL, Hess CP. Tips and tricks to optimize MRI protocols for cutaneous vascular anomalies. Clin Imaging 2017;45:71–80.
15. Mulligan PR, Prajapati HJ, Martin LG, Patel TH. Vascular anomalies: classification, imaging characteristics and implications for interventional radiology treatment approaches. Br J Radiol 2014;87(1035):20130392.
16. Raptis DA, Short R, Robb C, et al. CT appearance of pulmonary arteriovenous malformations and mimics. RadioGraphics 2022;42(1):56–68.
17. Henzler T, Vogler N, Lange B, et al. Low dose time-resolved CT-angiography in pediatric patients with venous malformations using 3rd generation dual-source CT: Initial experience. Eur J Radiol Open 2016;3:216–222.
18. Schmidt VF, Masthoff M, Czihal M, et al. Imaging of peripheral vascular malformations - current concepts and future perspectives. Mol Cell Pediatr 2021;8(1):19.
19. Green JR, Resnick SA, Restrepo R, Lee EY. Spectrum of imaging manifestations of vascular malformations and tumors beyond childhood: what general radiologists need to know. Radiol Clin North Am 2020;58(3):583–601.
20. Cartin-Ceba R, Swanson KL, Krowka MJ. Pulmonary arteriovenous malformations. Chest 2013;144(3):1033–1044.
21. Steiner JE, Drolet BA. Classification of vascular anomalies: an update. Semin Intervent Radiol 2017;34(3):225–232.
22. Lee HN, Hyun D. Pulmonary arteriovenous malformation and its vascular mimickers. Korean J Radiol 2022;23(2):202–217.
23. Kolarich AR, Solomon AJ, Bailey C, et al. Imaging manifestations and interventional treatments for hereditary hemorrhagic telangiectasia. RadioGraphics 2021;41(7):2157–2175.
24. Müller-Hülsbeck S, Marques L, Maleux G, et al. CIRSE standards of practice on diagnosis and treatment of pulmonary arteriovenous malformations. Cardiovasc Intervent Radiol 2020;43(3):353–361.
25. Yap CW, Wee BBK, Yee SY, et al. The role of interventional radiology in the diagnosis and treatment of pulmonary arteriovenous malformations. J Clin Med 2022;11(21):6282.
26. Asano Y, Tada A, Shinya T, et al. Utility of second-generation single-energy metal artifact reduction in helical lung computed tomography for patients with pulmonary arteriovenous malformation after coil embolization. Jpn J Radiol 2018;36(4):285–294.
27. Richter GT, Friedman AB. Hemangiomas and vascular malformations: current theory and management. Int J Pediatr 2012;2012:645678.
28. Hussein A, Malguria N. Imaging of vascular malformations. Radiol Clin North Am 2020;58(4):815–830.
29. Hammer S, Zeman F, Fellner C, Wohlgemuth WA, Uller W. Venous malformations: phleboliths correlate with the presence of arteriovenous microshunts. AJR Am J Roentgenol 2018;211(6):1390–1396.
30. Flis CM, Connor SE. Imaging of head and neck venous malformations. Eur Radiol 2005;15(10):2185–2193.
31. White CL, Olivieri B, Restrepo R, McKeon B, Karakas SP, Lee EY. Low-flow vascular malformation pitfalls: from clinical examination to practical imaging evaluation--part 1, lymphatic malformation mimickers. AJR Am J Roentgenol 2016;206(5):940–951.
32. Lee E, Biko DM, Sherk W, Masch WR, Ladino-Torres M, Agarwal PP. Understanding lymphatic anatomy and abnormalities at imaging. RadioGraphics 2022;42(2):487–505.
33. Gallagher JR, Martini J, Carroll S, Small A, Teng J. Annual prevalence estimation of lymphatic malformation with a cutaneous component: observational study of a national representative sample of physicians. Orphanet J Rare Dis 2022;17(1):192.
34. Olivieri B, White CL, Restrepo R, McKeon B, Karakas SP, Lee EY. Low-flow vascular malformation pitfalls: from clinical examination to practical imaging evaluation--part 2, venous malformation mimickers. AJR Am J Roentgenol 2016;206(5):952–962.
35. Lee S, Ko SY, Park WJ. Macrocystic lymphatic malformation of the chest wall and axilla: A case report in a 45-year-old man. Radiol Case Rep 2021;17(1):152–155. [Published correction appears in Radiol Case Rep 2023;18(4):1652.]
36. Martinez-Lopez A, Salvador-Rodriguez L, Montero-Vilchez T, Molina-Leyva A, Tercedor-Sanchez J, Arias-Santiago S. Vascular malformations syndromes: an update. Curr Opin Pediatr 2019;31(6):747–753.
37. Turner VL, Kearns C, Wattamwar K, McKenney AS. Klippel-Trenaunay syndrome. RadioGraphics 2022;42(6):E167–E168.
38. Bertino F, Braithwaite KA, Hawkins CM, et al. Congenital limb overgrowth syndromes associated with vascular anomalies. RadioGraphics 2019;39(2):491–515.
39. Léauté-Labrèze C, Harper JI, Hoeger PH. Infantile haemangioma. Lancet 2017;390(10089):85–94.
40. Hu PA, Zhou ZR. Clinical and imaging features of kaposiform hemangioendothelioma. Br J Radiol 2018;91(1086):20170798.
41. Lowe LH, Marchant TC, Rivard DC, Scherbel AJ. Vascular malformations: classification and terminology the radiologist needs to know. Semin Roentgenol 2012;47(2):106–117.
42. Navarro OM, Laffan EE, Ngan BY. Pediatric soft-tissue tumors and pseudo-tumors: MR imaging features with pathologic correlation: part 1. Imaging approach, pseudotumors, vascular lesions, and adipocytic tumors. RadioGraphics 2009;29(3):887–906.

43. Uno T, Ito S, Nakazawa A, Miyazaki O, Mori T, Terashima K. Successful treatment of Kaposiform hemangioendothelioma with everolimus. Pediatr Blood Cancer 2015;62(3):536–538.
44. Chinello M, Di Carlo D, Olivieri F, et al. Successful management of kaposiform hemangioendothelioma with long-term sirolimus treatment: a case report and review of the literature. Mediterr J Hematol Infect Dis 2018;10(1):e2018043.
45. Addula D, Das CJ, Kundra V. Imaging of Kaposi sarcoma. Abdom Radiol (NY) 2021;46(11):5297–5306.
46. Khalil AM, Carette MF, Cadranel JL, Mayaud CM, Bigot JM. Intrathoracic Kaposi's sarcoma. CT findings. Chest 1995;108(6):1622–1626.
47. Restrepo CS, Martínez S, Lemos JA, et al. Imaging manifestations of Kaposi sarcoma. RadioGraphics 2006;26(4):1169–1185.
48. Jang JK, Thomas R, Braschi-Amirfarzan M, Jagannathan JP. A review of the spectrum of imaging manifestations of epithelioid hemangioendothelioma. AJR Am J Roentgenol 2020;215(5):1290–1298.
49. Kitaichi M, Nagai S, Nishimura K, et al. Pulmonary epithelioid haemangioendothelioma in 21 patients, including three with partial spontaneous regression. Eur Respir J 1998;12(1):89–96.
50. Kim EY, Kim TS, Han J, Choi JY, Kwon OJ, Kim J. Thoracic epithelioid hemangioendothelioma: imaging and pathologic features. Acta Radiol 2011;52(2):161–166.
51. Crotty EJ, McAdams HP, Erasmus JJ, Sporn TA, Roggli VL. Epithelioid hemangioendothelioma of the pleura: clinical and radiologic features. AJR Am J Roentgenol 2000;175(6):1545–1549.
52. Wang H, Shi J, Liu H, et al. Clinical and diagnostic features of angiosarcoma with pulmonary metastases: A retrospective observational study. Medicine (Baltimore) 2017;96(36):e8033.
53. Fatima J, Duncan AA, Maleszewski JJ, et al. Primary angiosarcoma of the aorta, great vessels, and the heart. J Vasc Surg 2013;57(3):756–764.
54. Wu WH, Ji QL, Li ZZ, Wang QN, Liu SY, Yu JF. Mammography and MRI manifestations of breast angiosarcoma. BMC Womens Health 2019;19(1):73.
55. Gaballah AH, Jensen CT, Palmquist S, et al. Angiosarcoma: clinical and imaging features from head to toe. Br J Radiol 2017;90(1075):20170039.
56. Tan H, Jiang L, Gao Y, Zeng Z, Shi H. 18F-FDG PET/CT imaging in primary cardiac angiosarcoma: diagnosis and follow-up. Clin Nucl Med 2013;38(12):1002–1005.
57. Xi XY, Gao W, Gong JN, et al. Value of 18F-FDG PET/CT in differentiating malignancy of pulmonary artery from pulmonary thromboembolism: a cohort study and literature review. Int J Cardiovasc Imaging 2019;35(7):1395–1403.
58. Chen Y, Li Y, Zhang N, et al. Clinical and imaging features of primary cardiac angiosarcoma. Diagnostics (Basel) 2020;10(10):776.
59. Kaminaga T, Takeshita T, Kimura I. Role of magnetic resonance imaging for evaluation of tumors in the cardiac region. Eur Radiol 2003;13(Suppl 6):L1–L10.
60. Yoshihara S, Sugimoto Y, Matsunaga M, Suzuki S, Tanioka F. Coronary vessel floating sign in cardiac diffuse large B-cell lymphoma. Eur Heart J Cardiovasc Imaging 2020;21(2):233.